PAPER • OPEN ACCESS

The experimental analysis of creep and corrosion properties of polymeric tube reinforced by glass, carbon and Kevlar fibers

View the article online for updates and enhancements.

IOP ebooks™

Bringing together innovative digital publishing with leading authors from the global scientific community.

Start exploring the collection−download the first chapter of every title for free.

Materials Research Express

The experimental analysis of creep and corrosion properties of polymeric tube reinforced by glass, carbon and Kevlar fibers

Kaveh Rahmani[1] , Greg Wheatley[2], Ali Sadooghi[3] , Seyed Jalal Hashemi[4] and Jafar Babazadeh[5]

1 Department of Mechanical Engineering, Bu-Ali Sina University, Hamedan, Iran
2 College of Science & Engineering, James Cook University, James Cook Dr, Douglas QLD 4811, Australia
3 Department of Mechanical Engineering, Faculty of Enghelab-e Eslami, Technical and Vocational University (TVU), Tehran, Iran
4 Department of Mechanical Engineering, Kar Higher Education Institute of Qazvin, Qazvin, Iran
5 Department of Mechanical Engineering, Shahid Rajaee Teacher Training University, Tehran, Iran

E-mail: rahmanii.kaveh@gmail.com

Abstract

Polymeric tubes, including epoxy and reinforcing fibers, are widely used in the petroleum and aerospace industries due to their high strength and corrosion resistance. In this study, corrosion and creep properties of resin-based tubes reinforced by Glass fibers (GFR), Carbon fibers (CFR), and Kevlar fibers (KFR) were investigated using tubes made by using a 45-degree unilateral winding method. The highest creep strain was obtained for the CFR equal to 0.7445 and the lowest was obtained for KFR with the Kevlar fibers being severely damaged. The lowest corrosion rate per year was for the CFR sample, equal to 113in/year×1000. The corroded samples were subjected to a tensile test and a 2% improvement in ultimate tensile strength was achieved for GFR. To evaluate the results and the quality of adhesions between fibers and resins, SEM images were taken of the samples.

1. Introduction

There has been significant research concerning polymeric composite materials in which fibers are used to reinforce resins which are thermoset or thermoplastic polymers [1, 2]. These materials have a high strength to weight ratio and their significant properties include high tensile strength, flexural strength, fatigue life, and corrosion resistance [3]. The properties of polymeric composites depend on the polymer properties as well as on the type, direction, and length of the fibers and the quality of resin and fiber bonding [4]. The fibers transfer stress from the polymer matrix to themselves, reduce the stress concentration and improve the sample's toughness [5]. Also, composite tubes, due to their durable, corrosion-resistant, and lightweight structure are a great alternative to metal and concrete pipes [6]. In addition, the inner surface of the composite tube is very smooth which reduces energy consumption, pressure drop, sedimentation, and the friction coefficient that allows it to not require a pipe protection cover against corrosive fluids and environmental factors [7]. Apart from the type and arrangement of the fibers, the properties of composite tubes depend on the compatibility and interleaving between fibers and resin matrix [8]. An incompatible resin, lack of bonding, and weak adhesion strength lead to delamination and failure of fiber-reinforced materials [9]. Experimental and laboratory trial-and-error is the most commonly adopted strategy to validate the performance and determine the compatibility of fiber reinforcement materials [10]. Many kinds of research have been done on the energy absorption or creep and corrosion behavior of fiber-reinforced composite samples [11, 12].

Liu *et al* [13] produced carbon fiber reinforced polymer tubes and the transverse impact test was done on the samples with their failure mechanisms investigated. The results show that higher impact energy led to more circumferential cracks. Also, by increasing the impact energy, the tubes absorbed energy by generating circumferential and longitudinal cracks. Wang *et al* [14] investigated the corrosion behavior and durability of concrete-filled fiber-reinforced polymer tubes subjected to the various conditions with additional sustained axial load and continuous water immersion. Test results showed that more degradation occurred for wet
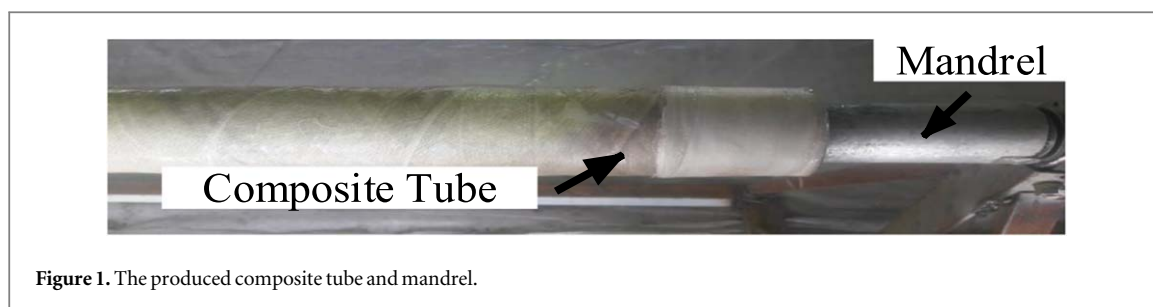
Figure 1. The produced composite tube and mandrel.

Table 1. The detailed specification of used fibers.

Fiber	Structure	Thickness (μm)	Density (g/cm^3)	Modulus of elasticity (GPa)	Break elongation (%)	Specific tensile strength (Glb/in^2)
Glass	Plain Woven	10	2.54	72.39	4.8	5.43
Carbon	Plain Woven	15	1.79	220.63	1.4	6.93
Kevlar49	Plain Woven	15	1.43	112.38	2.4	7.38

Table 2. The feature and arrangements of fibers for production tubes.

Sample	Inner Layer		Middle Layer		Outer Layer	
	Material	Mark	Material	Mark	Material	Mark
GFR	Glass Fiber	Mat225	Glass Fiber	Woven 600	Glass Fiber	Mat225
CFR	Fabric	Re300	Carbon Fiber	300	Fabric	Re300
KFR	Fabric	Re300	Kevlar Fiber	49	Fabric	Re300

conditions compared to the dry environment. Ren *et al* [15] did a compression test at various temperatures and pressures on shape memory polymer composite tube reinforced by carbon fibers wound with $\pm 45°$ layers. The results showed that increased compression resulted in less buckling load. Yang *et al* [16] did an experimental analysis on the creep behavior of composite tubes under flexural loading. The flexural creep test was done at various stress, 45% to 75% of ultimate flexural strength at 100 °C for 500 h, and the tubes' deformation, mechanical performance, and service reliability were evaluated by the superposition principle after a 12-year design life.

Acquiring knowledge of the corrosion and creep properties of fiber-reinforced composite tubes according to compatibility role can help extend their application in various industries, in which little research has been done so far. In this paper, composite tubes with polymer base material were reinforced by glass, carbon, and Kevlar fibers with a unilateral winding at an angle of 45 degrees. Another main aim and the novelty of this study is that it considers the compatibility of fibers and resins. In this study, a corrosion test in an acidic environment and a creep test were done on tubes. Finally, SEM images were taken on the samples to validate the results.

2. Experimental part

2.1. Materials and producing tubes

To obtain high-quality samples with reinforcing fibers, a suitable resin material was used. The resins used for manufacturing with GFR, CFR, and KFR are Swancor-901, Epiran-10, and Epiran-06FL types, respectively, which were achieved by trial-and-error in our previous research [1]. Two additives such as cobalt actuate and peroxide acid solutions were added to the resin at 1.5% and 15% by weight, respectively, which facilitates the curing process [17]. After preparing the resin, the fibers were immersed in the resin solution for 20 min (Gel time). The detailed specifications according to the producers' datasheet of the fibers can be seen in table 1. To produce composite tubes, a shaft with a 26 mm diameter, called a mandrel, was used and placed in the winding machine. To ensure proper adhesion of the fibers to the mandrel and smoothness of the surface, the mandrel was polished first, and a very thin layer of resin called gel coat was sprayed with a thickness of 0.7 mm. Table 2 presents the specifications and layering fibers of the tubes.

After wrapping impregnated fibers around the mandrel, the samples were placed for 2 h at ambient temperature for initial curing and then were placed in an oven for 2 h at 70 °C for final curing. Figure 1 shows the produced tube and, their average characteristics are given in table 3.
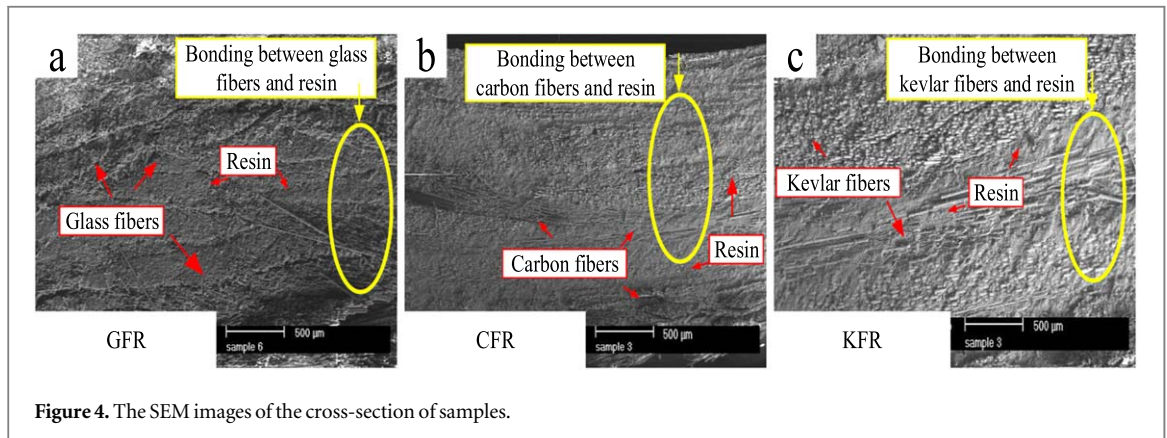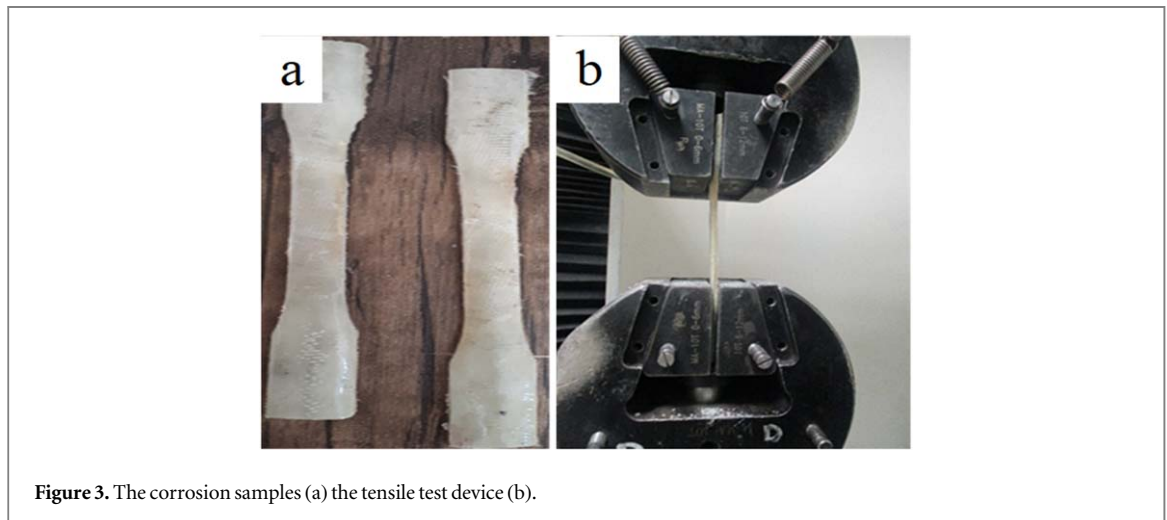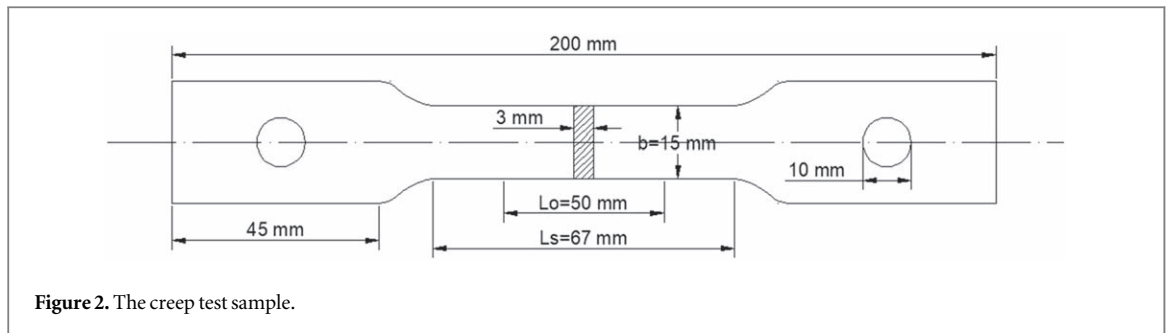
Figure 2. The creep test sample.

Figure 3. The corrosion samples (a) the tensile test device (b).

Figure 4. The SEM images of the cross-section of samples.

Table 3. The specification of the produced tubes.

Sample	Thickness (mm)	Diameter (mm)	Mass per 20 cm (g)	Density (g/mm^3)
GFR	3.34	33.4	79	1.252
CFR	3.34	33.4	75	1.189
KFR	3.34	33.4	78	1.237

2.2. Determining mechanical properties

The creep test was performed on samples at 50 MPa stress and 200 °C, according to the ASTM-D7337 standard [18] and the increase in length and strain of the samples were measured until rupture point. The creep samples were cut from the produced tube and a schematic image of them is presented in figure 2.

For the corrosion test, the samples were first polished with a grade 3000 emery and dried for 120 min at 50 °C. The test was carried out according to ASTM-C582 standard in 37% concentration acidic HCl solution [19]. The samples were exposed to acid for 24 h at 40 °C and the corrosion rate was calculated according to

Figure 5. The TGA graph of the produced samples.

Figure 6. The Creep graph of produced tubes.
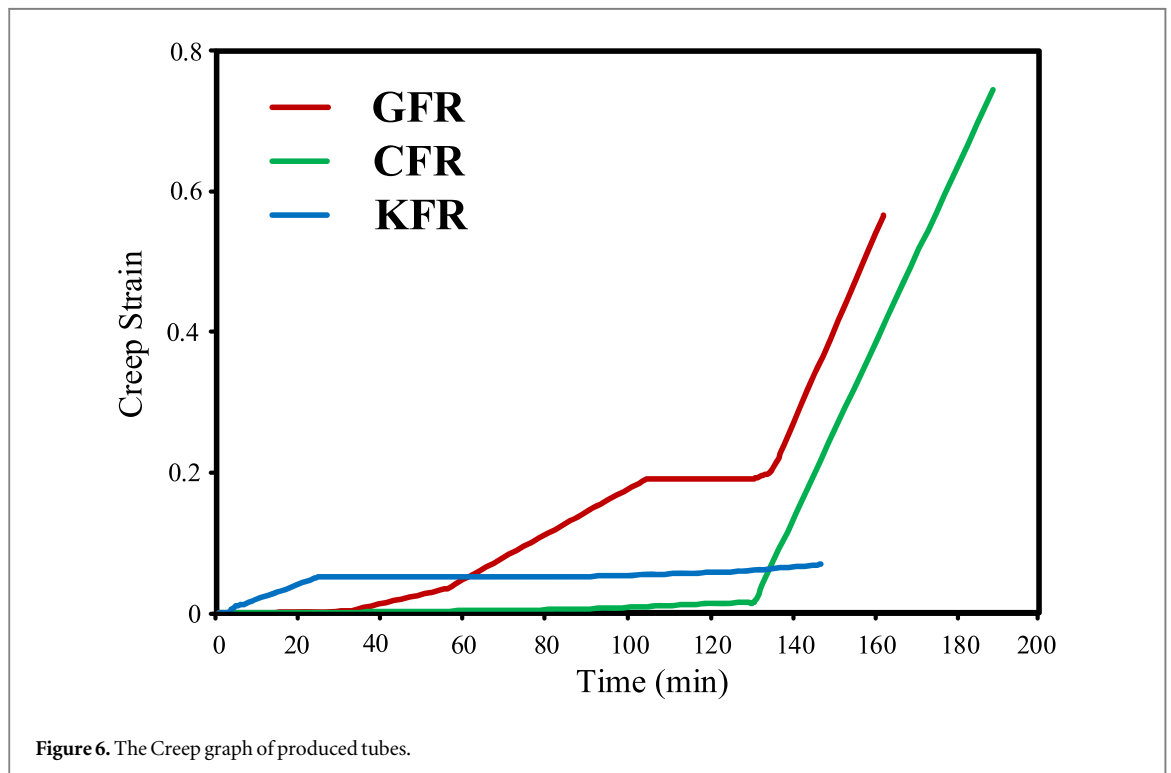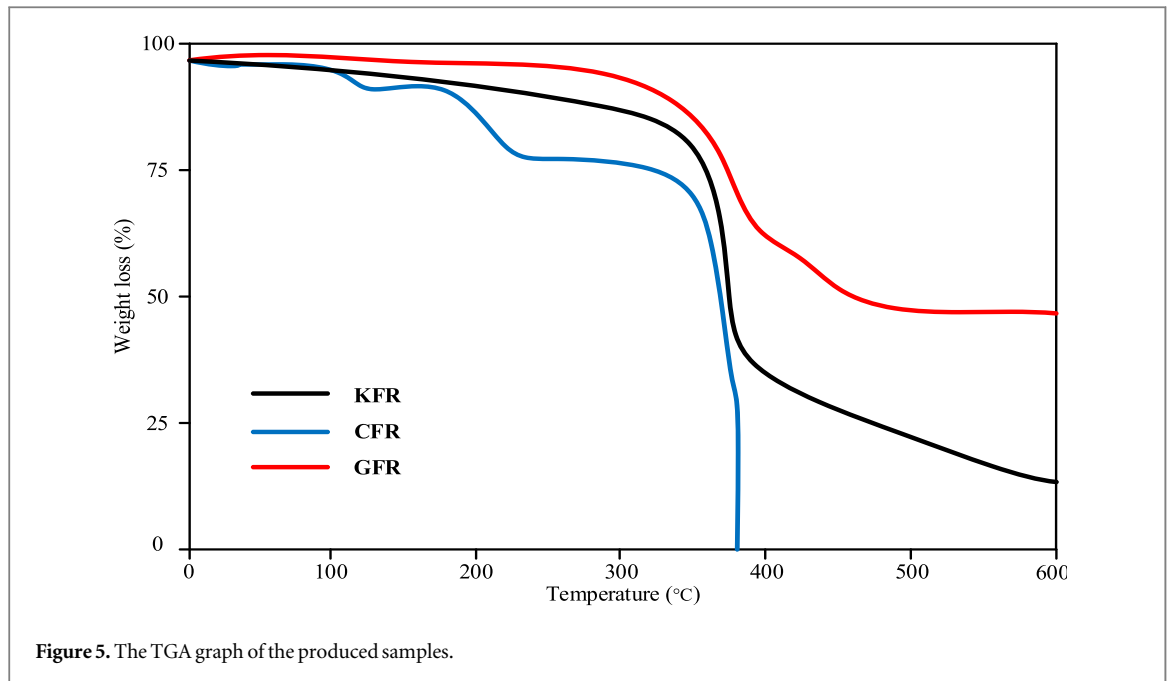
equation (1) where W, D, A, T are lost mass (mg), density (g/cm^3), area (in^2), and time (hour), respectively. Before and after the corrosion test, the tensile test was performed on the samples according to the ASTM-D638 standard with 50 mm gauge length, 5 mm min^{-1} force speed, and 0.001 s^{-1} strain rate [20]. The images of the corrosion samples and the tensile test device are shown in figure 3.

$$mpy = 543 * W/D * A * T \tag{1}$$

3. Results and discussion

3.1. Specification of samples

To ensure the quality of adhesion and compatibility between resins the fibers, SEM imaging was done at the cross-sectional area of the samples. Figure 4, shows these SEM images and the fibers between resins have been
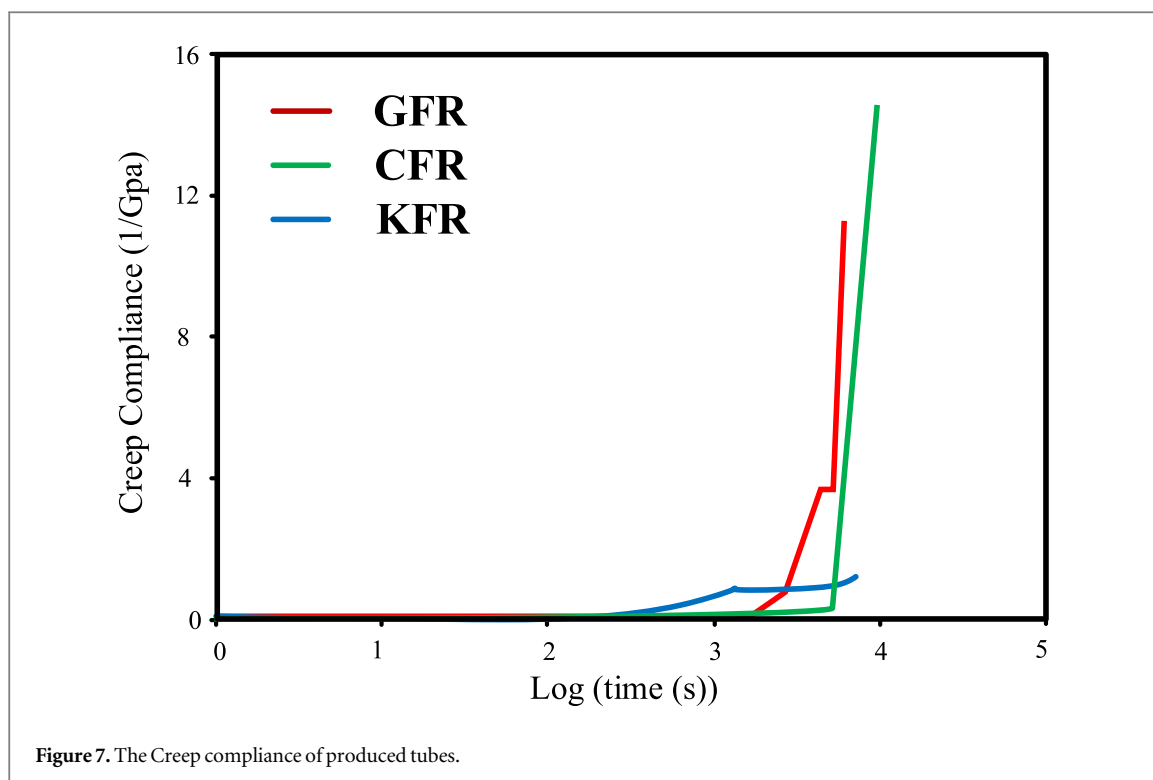
Figure 7. The Creep compliance of produced tubes.

Table 4. The result of the creep test.

Sample	Initial length (cm)	Final length (cm)	Time (min)	Max. of creep strain
GFR	20	28.37	152	0.584
CFR	20	34.89	190	0.7445
KFR	20	21.3819	148	0.0691

identified, and the bonding between them is plotted, with no discontinuities, porosities, or cavities, which are common defects in fiber reinforcement samples. Also, the TGA test was done on samples to study the thermal stability and weight loss of the samples by increasing temperature [21]. TGA analysis can provide valuable information regarding the composition and thermal stability of polymeric materials. This can be done to compare different materials or through accelerated means for lifetime predictions [22]. The TGA curve of produced samples can be seen in figure 5. The degradation in the samples can be accomplished by processes such as cross-linked breakages due to the increasing temperature. For all produced samples, the degradation occurred at about 330 °C. By using carbon fibers, 20%, and 8% higher degradation have been achieved compared to the samples in which glass and Kevlar fibers were used, respectively. These results were obtained due to the better thermal stability of carbon fibers compared to other tested fibers, and appropriate compatibility and bonding between reinforcement fibers and resins. Mass changes at sample temperatures between 250 °C and 300 °C can be correlated to changes in molecular structure and is believed to reflect the extent of matrix depolymerization which may have occurred [22].

3.2. The creep test

The tensile creep test was performed on the samples and the strain data was extracted from the device until the complete rupture of samples. The results of the creep test of the composite tube can be seen in table 4. Creep in polymer composites may occur at any temperature, even at low temperatures, due to the viscoelastic deformation of the base material, although normally the fibers do not creep at this temperature and the creep behavior of the composites is influenced by the geometry of the segment and the properties of their constituents.

To investigate the creep behavior of fiber-reinforced polymers, creep compliance (D(t)) can be used [23], which is defined by equation (2). In this equation, $\varepsilon(t)$ is the instantaneous strain, and σ_0 is the constant stress applied to the samples. The strain changes over time and the D(t) values for produced samples with different
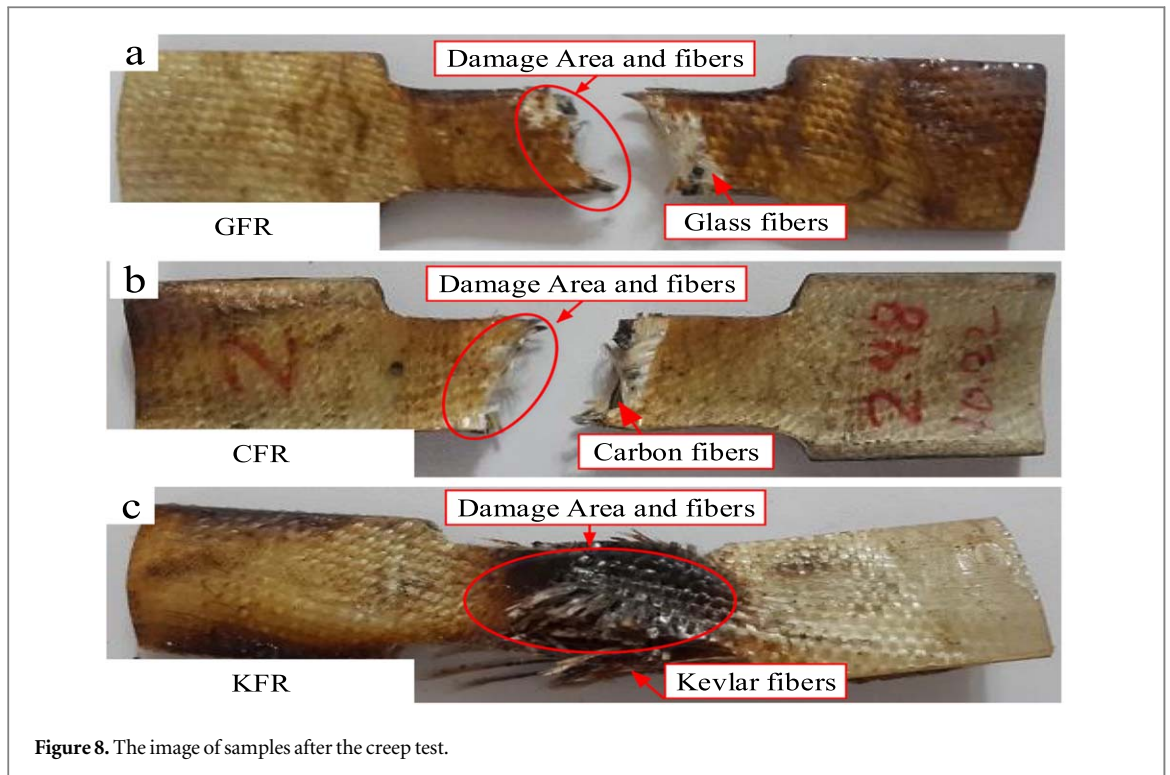
Figure 8. The image of samples after the creep test.
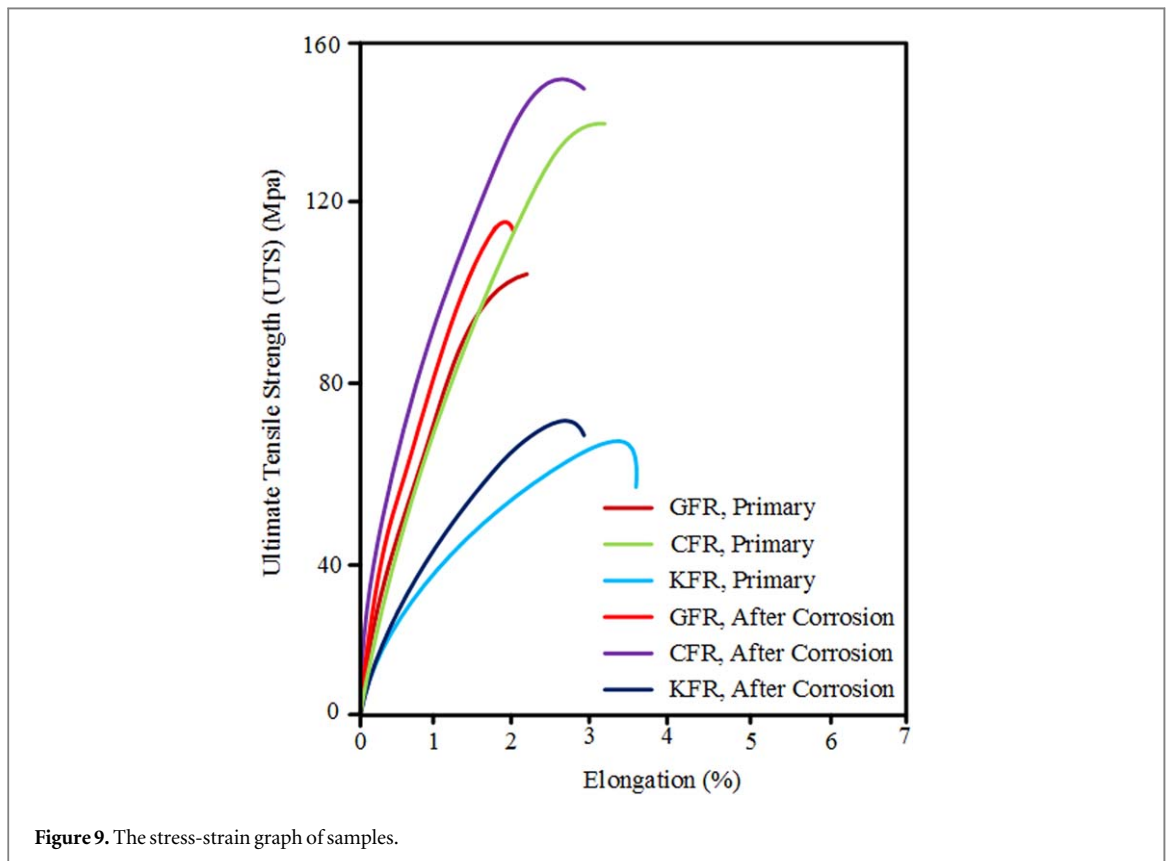
Figure 9. The stress-strain graph of samples.

reinforcing fibers are shown in figures 6 and 7, respectively.

$$D(t) = \frac{\varepsilon(t)}{\sigma_0} \qquad (2)$$

According to the obtained results, variations of the creep compliance are linear for all samples and the highest creep strength up to 133 min was related to CFR, which did not show much deformation. The abrupt change of the diagrams corresponds to the time when the fibers were separated from the base material, or the

Table 5. The results of the corrosion test.

Sample	Area (cm^2)	Density (g/cm^3)	Initial mass (mg)	Final mass (mg)	Loss mass (mg)	Loss mass (%)	Corrosion rate (in/ year × 1000)
GFR	49	1.72	930	917.70	12.30	1.3	142
CFR	49	1.61	450	445.72	4.28	0.9	113
KFR	49	1.52	734	718.76	15.24	2	275

Table 6. The result of the tensile test before and after corrosion test.

Sample	Ultimate tensile strength (MPa), Primary	Ultimate tensile strength (MPa), After corrosion	Elongation (%), Primary	Elongation (%), After corrosion
GFR	109.5	111.7	2.17	1.95
CFR	139	140.8	3.35	2.96
KFR	58.7	59.25	3.41	2.90

composite layers were delaminated. After the mentioned time (133 min), the abrupt separation between the carbon fibers and the resin occurred, followed by the creep stress only carried by the carbon fibers, which is illustrated by the slope of the diagram. In the case of GFR, the separation of the layers was first observed at times of 60 min and 104 min, respectively. Then at 128 min, the fibers started to separate from the base material, and finally, the fibers were ruptured so that, the creep compliance diagram for GFR also shows the slope change, which confirms this. In the case of KFR, the separation of the layers occurred slower, but eventually, the rupture of the sample occurred earlier than the CFR and GFR. The difference in the stress transfer mechanism in the samples is due to the difference in the creep rupture behavior of the samples. Also, to investigate the behavior of the fibers against the applied stress and heat, the images of samples are visible in figure 8. Examination of the surface of the samples revealed that the outer layers of the fibers broke down earlier, and then the inner layers in the middle of the composite were fractured. At the beginning of loading, the stress was tolerated by the fibers in all layers. After exposure to heat, the temperature affects the outer layers and causes submission in these layers. This causes more stress to be applied to the inner layers, and then, after the outer layers failed, the inner layers were exposed to higher temperatures that eventually led to their failures. This indicates that each layer was ruptured at different times.

As can be seen in figure 8, there is good agreement with the results. The GFR and CFR had a similar process until destruction, and all layers failed at approximately the same time. In these samples, the fibers were less damaged due to their higher temperature tolerance; and in the GFR, more severe destruction occurred compared to CFR. In the KFR, considering that the temperature tolerance of these fibers is much lower than the other two fibers, the fibers of the outer Kevlar fibers have been severely damaged, resulting in early damage to the sample at lower strain times and rates.

3.3. The tensile strength of corroded samples

To evaluate the produced samples' resistance to an acidic solution, the corrosion test was performed. The corrosion test results for composite tubes are visible in table 5. The lowest corrosion rate per year was obtained for CFR, equal to 113 in/1000 × year, which is 134% lower than KFR. In general, the base material, resin, has a higher corrosion resistance than metal and steel samples due to its lower reactivity and absorption of corrosive materials [24]. These materials also prevent osmotic blistering and are used as insulating material against corrosive materials; they have higher thermal and chemical resistance and less water absorption [25]. To determine the effect of the acidic environment on produced composite samples, the uniaxial tensile test was performed on samples before and after the corrosion test. The maximum tensile strength of the samples and their results are shown in table 6. The results show that the tensile strength of the produced samples increased after the corrosion test, and their fracture strain decreased, which were similar to obtained results in the previous literature [26, 27]. The tensile strength of the samples depends on the reinforcing fibers, which prevent growth in the rupture.

The acidic environment creates a better bond and interaction between the base material and the reinforcing fibers by treatment aging under acidic conditions [27]. The highest change in the ultimate tensile strength after corrosion was obtained for sample GFR, equal to 111.7 MPa, with a 2% improvement. On the other hand, acidic corrosion had the least effect on CFR, which is consistent with the high resistance of carbon fibers to acidic environments [28]. After corrosion testing, the fracture strain of all samples decreased; The highest change in the amount of reduction was obtained for GFR, equal to 2.5%. To better understand the results of the tensile test, the stress-strain graphs of the samples are shown in figure 9.

4. Conclusion

In this study, epoxy tubes were reinforced with glass, carbon, and Kevlar fibers with the unidirectional winding method, and their corrosion rate and creep behavior were evaluated.

1. For all samples, the degradation occurred at about 330 °C. By using carbon fibers, 20%, and 8% higher degradation have been achieved compared to the samples reinforced by glass and Kevlar fibers, respectively.

2. The KFR had the lowest creep strain, and its fibers were severely damaged. In contrast, CFR had the highest strain rate, equal to 0.7445.

3. The corrosion test results showed that the lowest corrosion rate was for sample CFR, equal to 113in/year×1000, which is 143% lower than KFR.

4. The highest change in ultimate tensile strength after the corrosion test was obtained for GFR, equal to 111.7 MPa, with a 2% improvement. After corrosion testing, the fracture strain of all samples decreased, the biggest change in the amount of reduction was for GFR, equal to 2.5%.

Data availability statement

All data that support the findings of this study are included within the article (and any supplementary files).

ORCID iDs

Kaveh Rahmani ⓘ https://orcid.org/0000-0002-0815-1562
Ali Sadooghi ⓘ https://orcid.org/0000-0001-5169-7790

References

[1] Babazadeh J *et al* 2021 Effect of glass, carbon, and kevlar fibers on mechanical properties for polymeric composite tubes produced by unidirectional winding method. *Mater. Res. Express* **8** 045301

[2] Hashemi S J *et al* 2020 Investigation on the mechanical behavior of fiber-metal laminates based on polyvinyl chloride reinforced by 3D glass fibers *Materials Today Communications* **25** 101273

[3] Daniel I M *et al* 1994 *Engineering Mechanics of Composite Materials.* vol 3 (New York: Oxford University Press)

[4] Akram W, Chaturvedi S K and Ali S M 2013 Comparative study of mechanical properties of e-glass/epoxy composite materials with Al_2O_3, $CaCo_3$, SiO_2 AND PBO fillers *International Journal of Engineering Research & Technology* **2** 1029–34

[5] Ansari E *et al* 2018 The effect of middle layer material and thickness on the quasi-static energy absorption of FML *Journal of Science and Technology of Composites* **5** 427–36

[6] Pazilarasu V and Perameshwaranpillai T 2013 Comparison of performance of glass fiber reinforced plastic leaf spring with steel leaf spring *International Journal Of Chem. Tech Research* **5** 1339–45

[7] Ramnath B V *et al* 2013 Evaluation of mechanical properties of abaca–jute–glass fibre reinforced epoxy composite *Mater. Des.* **51** 357–66

[8] Gunge A, Koppad P G, Nagamadhu M, Kivade S B and Murthy K V S 2019 Study on mechanical properties of alkali treated plain woven banana fabric reinforced biodegradable composites *Composites Communications* **13** 47–51

[9] Ren M *et al* 2020 Molecular investigation on the compatibility of epoxy resin with liquid oxygen *Theoretical and Applied Mechanics Letters* **10** 38–45

[10] Panduranga R, Matthew M S and Kunigal N S 2012 Assessment of polymer nanofiber interleaving in composite laminates through simple tests *Int. SAMPE technical conference*

[11] Liu M *et al* 2020 Crashworthiness of thermoplastic woven glass fabric reinforced composite tubes manufactured by pultrusion *Fibers Polym.* **21** 416–27

[12] Chambe J-E *et al* 2019 Energy absorption capacity of composite thin-wall circular tubes under axial crushing with different trigger initiations *J. Compos. Mater.* **10** 1281–304

[13] Liu Y, Zhuang W and Wu D 2020 Performance and damage of carbon fibre reinforced polymer tubes under low-velocity transverse impact *Thin-Walled Structures* **151** 106727

[14] Wang S and Mohamed A E G 2019 Effects of hybrid water immersion, environmental exposures, and axial load on the mechanical properties of concrete filled epoxy-based glass fiber reinforced polymer tubes *Constr. Build. Mater.* **194** 311–21

[15] Ren Z *et al* 2020 Damage and failure in carbon fiber-reinforced epoxy filament-wound shape memory polymer composite tubes under compression loading *Polym. Test.* **85** 106387

[16] Yang Z *et al* 2018 Flexural creep tests and long-term mechanical behavior of fiber-reinforced polymeric composite tubes *Compos. Struct.* **193** 154–64

[17] Vinay H B, Govindaraju H K and Banakar P 2014 A review on investigation on the influence of reinforcement on mechanical properties of hybrid composites *International Journal of Pure & Applied Sciences & Technology* **24** 2

[18] ASTM D7337 / D7337M-12 2019 *Standard Test Method for Tensile Creep Rupture of Fiber Reinforced Polymer Matrix Composite Bars* (West Conshohocken, PA: ASTM International) www.astm.org

[19] Rahmani K, Sadooghi A and Hashemi S J 2020 The effect of Al_2O_3 content on tribology and corrosion properties of Mg-Al_2O_3 nanocomposites produced by single and double-action press *Mater. Chem. Phys.* **7** 123058

[20] ASTM D638-14 2014 *Standard Test Method for Tensile Properties of Plastics* (West Conshohocken, PA: ASTM International)
      www.astm.org

[21] Hashemi S J *et al* 2020 Experimental determining the mechanical and stiffness properties of natural rubber FRT triangle elastic joint
      composite reinforcement by glass fibers and micro/nano particles *Polym. Test.* **85** 106461

[22] Salvador M ª D *et al* 2004 Thermal analysis of polymer resin matrix reinforced with E-glass fibers degradated in neutral environment.
      Proc. of 11th European Conference on Composite Materials

[23] Dean G 2007 Modelling non-linear creep behaviour of an epoxy adhesive *Int. J. Adhes. Adhes.* **27** 636–46

[24] Mouritz A P *et al* 2001 Review of advanced composite structures for naval ships and submarines *Compos. Struct.* **53** 21–42

[25] Roseman M, Martin R and Morgan G 2016 Composites in offshore oil and gas applications *Marine Applications of Advanced Fibre-
      Reinforced Composites* (Sawston: Woodhead Publishing) pp 233–57

[26] Stamenović M *et al* 2011 Effect of alkaline and acidic solutions on the tensile properties of glass–polyester pipes *Mater. Des.* **32** 2456–61

[27] Sindhu K *et al* 2007 Degradation studies of coir fiber/polyester and glass fiber/polyester composites under different conditions *J. Reinf.
      Plast. Compos.* **26** 1571–85

[28] Pritchard G and Henson J H L 1971 Carbon-fibre paper—an anti-corrosion material *Composites* **2** 38–40